

# Evidence for Defect Pairs in SiON pMOSFETs

T. Grasser\*, K. Rott†, H. Reisinger†, M. Waltl\*, and W. Goes\*

\*Institute for Microelectronics, TU Wien, Vienna, Austria

†Infineon, Munich, Germany

**Abstract**—Detailed time-dependent defect spectroscopy (TDDS) studies have recently demonstrated that recovery following negative bias temperature stress in MOSFETs is to good approximation consistent with a collection of independent (effective) first-order reactions. While the data are largely consistent with the first-order picture, several ‘anomalies’ such as switching traps and disappearing/reappearing traps have already been identified and analyzed. Here, we focus on a newly made observation, namely that emission events apparently belonging to a single defect can in fact be composed of two subsequent emission events if the device is stressed for a long enough time. We analyze this peculiarity as a function of bias and temperature and conclude that it is most likely due to a pair of defects which for some reason have similar configurations and thus similar properties.

## I. INTRODUCTION

Using the recently introduced time-dependent defect spectroscopy (TDDS) [1], recovery of the negative bias temperature instability (NBTI) has been extensively studied at the single defect level [2–7]. These studies have shown that NBTI recovery can be well described by assuming a collection of independent (effective) first-order reactions with widely distributed reaction rates, or, alternatively, capture and emission times. At closer inspection, as is the case for many complicated systems, the reactions appear first-order only under certain circumstances, since metastable defect states have a fundamental impact on the dynamics. In particular, these metastable states explain the difference between fixed positive vs. switching traps [8], the decorrelation between capture and emission times as well as their frequency dependence [9]. Also, temporary random telegraph noise (tRTN) stimulated by NBTI stress [1] can only be understood with metastable states [10]. Furthermore, defects have been observed to disappear and reappear during subsequent stress and recovery cycles on a wide range of timescales, suggesting the involvement of hydrogen [11].

Here, we look at a newly observed anomaly, namely the occurrence of two emission events inside a single trace with nearly identical statistics. These statistics will be analyzed and discussed as a function of bias and temperature and then contrasted with three possible explanations.

## II. EXPERIMENTAL METHOD

In a TDDS setup, a nanoscale device is repeatedly stressed and recovered (say  $N = 100$  times) using fixed stress/recovery times,  $t_s$  and  $t_r$ . The recovery trace is analyzed for discrete steps of height  $\eta$  occurring at time  $t_e$ . Each  $(\eta, t_e)$  pair is then placed into a 2D histogram, which we call spectral

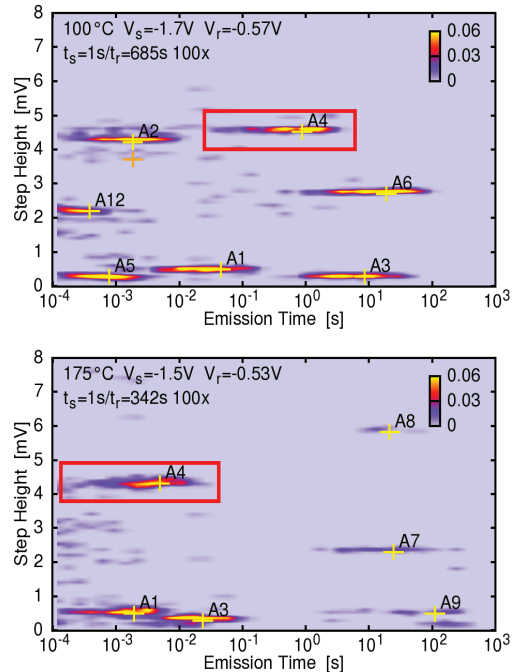


Fig. 1: The spectral map of device A of [1, 8] at 100 °C (top) and 175 °C (bottom). From the visible defects, for longer stress times only defect A4 contains two emission events from a single trace. This feature is maintained at different temperature and different voltages, implying that this is not simply due to a coincidental overlap of two defects. Note how defects have different activation energies, implying a different relative ‘movement’ on the map with changing temperature. Also note that defect A6 has disappeared from the map in the bottom figure.

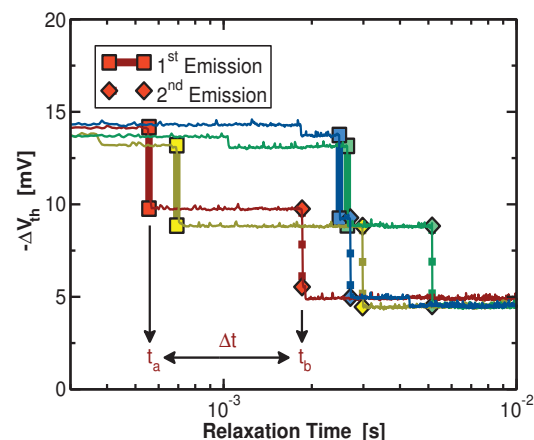


Fig. 2: Typically, in each trace only a single emission event is observed per cluster. However, particularly for larger stress times, two emission events can sometimes be observed. Here, four example traces contributing to the 175 °C spectral maps of Fig. 1 are shown. The step-heights of the second emission event are within 5% of those of the first emission event. Note that the emission events  $t_a$  and  $t_b$  do not directly correspond to the emission times of the defects as discussed below.

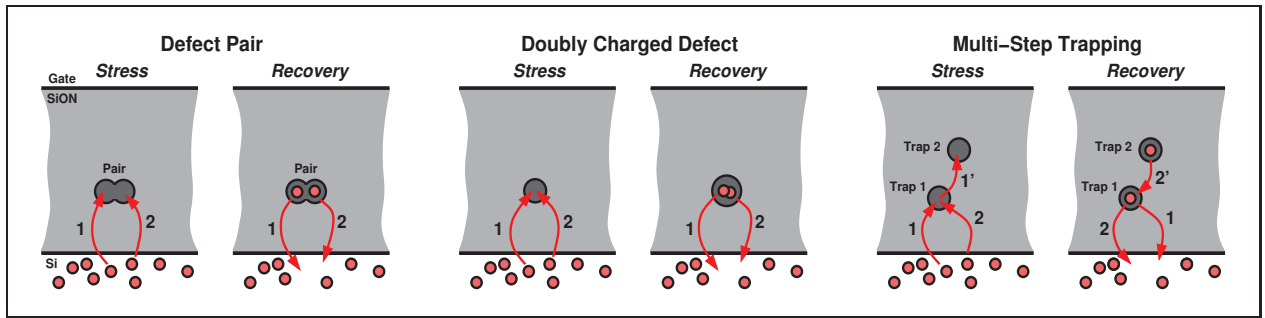


Fig. 3: **Left:** Scenario A: in a certain defective region of the oxide two holes can be trapped subsequently, with the second capture having a larger time constant. A similar configuration is required to explain the same emission time for both emission events. **Middle:** Scenario B: A defect may be able to subsequently capture two holes. **Right:** Scenario C: In a three-step process, a hole is first captured (1), then moves deeper into the oxide (1'), which allows capture of a second hole (2). Emission proceeds in reverse order but always from the same defect, which could explain the similar emission times.

map, see Fig. 1 for examples. The clusters forming in the spectral maps reveal the probability density distribution and thus provide detailed information on the statistical nature of the trap annealing time constant  $\tau_e$ . We remark that the TDDS only detects the change of the charge state of individual defects, and as such cannot directly differentiate e.g. between the emission of charges from oxide states or the annealing of interface states. Nevertheless, so far, only exponentially distributed emission/annealing events (analyzed on a logarithmic scale) have been observed for the emission events  $t_e$ ,

$$f(\eta, t_e) = f_\eta(\eta) \frac{t_e}{\tau_e} \exp\left(-\frac{t_e}{\tau_e}\right) \quad (1)$$

which is consistent with independent first-order processes. Due to noise, the step-heights  $\eta$  are typically Gaussian distributed around an exponentially distributed mean  $\bar{\eta}$ . However, defects may interact electrostatically [1], leading to multiple peaks in the  $f_\eta$  distribution. As such, the extraction of the  $(\eta, t_e)$  pairs is sensitive to noise, particularly RTN, and a certain (hard to quantify) error larger than the typical  $\Delta\tau_e = \pm\tau_e/\sqrt{N}$  has to be expected. Furthermore, clusters in the spectral map of the form given by (1) may partially overlap, leading to the erroneous detection of  $(\eta, t_e)$  pairs and assignment to the ‘wrong’ defect. Still, at not too high stress voltages and not too large stress times, the accuracy is typically very high, and the bias and temperature dependence of  $\bar{\eta}$  and  $\tau_e$  can be easily extracted.

### III. REFINED DATA ANALYSIS

At closer inspection of the extraction error in the  $(\eta, t_e)$  pairs we noticed that in some defects two emission events which apparently belong to the same cluster can occur in a single trace. These emission events occurred with a regularity clearly beyond any extraction errors and were investigated in closer detail. Roughly, about 10-20% of the defect clusters in three devices investigated belong to this category. One example, defect A4 (defect #4 of device A previously studied [1]), is shown in Fig. 1. At a first glance, the cluster looks perfectly regular as expected from (1). However, it occasionally contains two emission events from a single recovery trace, inconsistent with (1), see Fig. 2. This phenomenon is observed for all

temperatures studied (100 °C – 175 °C), not too low biases ( $\gtrsim V_{DD} = -1.3$  V, on a SiON device [12] with EOT=2.2 nm and  $V_{th} = -0.7$  V), starting from stress times about a 1,000 times larger than the capture time of the cluster that produces the first emission event.

The *trivial* explanation for such double emissions, namely that two independent defects by fortuitous coincidence just happen to have the same step-heights and emission times, can be ruled out based on several considerations:

- (i) the spectral maps are only scarcely populated and the probability that two defects have the same parameters within experimental resolution is about  $10^{-4}$  (assuming a log-uniform  $\tau_e$  and an exponential  $\bar{\eta}$  distribution).
- (ii) All defects have quite a distinct bias and temperature dependence, and as will be shown below, variation of these parameters does not lead to a separation of these clusters.
- (iii) Finally, even in the extremely unlikely case that such a pair of defects should exist in one device, the occurrence of such pairs in the other two devices investigated appears highly unlikely.

Therefore, to go beyond the trivial explanation, three possible scenarios to explain such a behavior are considered, see sketches in Fig. 3. For the analysis of the experimental data we have to distinguish between the *physical processes* underlying the double hole emission events from *what is recorded* by TDDS. For example, if we have two defects with identical emission times and step-heights, we will have a 50% probability that the first emission event belongs to defect 1, while the other 50% will belong to defect 2.

#### A. Scenario A: Defect Pair

In scenario A we assume that we are dealing with two defects which are spatially close but otherwise (nearly) independent. This is based on the assumption that defects may be more likely in certain defective areas of the oxide, as also recently suggested for the case of dielectric breakdown [13]. Then, the two holes are emitted at independent random times  $t_1$  and  $t_2$ , while TDDS will see the first event at  $t_a = \min(t_1, t_2)$  and the second at  $t_b = \max(t_1, t_2)$ . If the emission

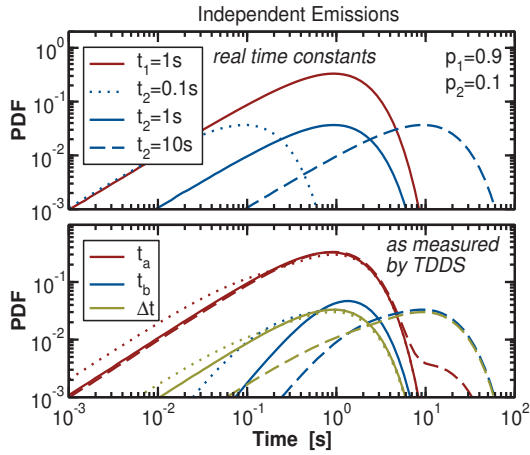


Fig. 4: Scenario A: **Top**: The (real) time constants of the two defects independently emitting a hole. The first emission time is fixed to 1 s while the second is varied from 0.1 s to 10 s (dotted/solid/dashed curves). Typical capture probabilities  $p_1 = 0.9$  and  $p_2 = 0.1$  are used. **Bottom**: The simulated distribution of the first emission event  $t_a$  recorded by TDDS is close to exponential, dominated by  $\tau_1 = 1$  s, with only a small modulation at short and large times, which is outside our experimental resolution. The distribution  $t_b$  of is narrower than exponential. Most importantly, the distribution of  $\Delta t$  is similar to that of the first event  $t_a$ .

times  $t_1$  and  $t_2$  are exponentially distributed, the distributions of  $t_a$  and  $t_b$  can easily be calculated. For this we also need to consider that the probabilities of having either of these emission events are not equal and depend on the probability of having captured a charge in either defect. Experimentally, we typically see mostly emission events related to the first hole for shorter stress times while double emissions are only recorded for larger times. We consider this fact by taking different capture probabilities  $p_i$  of the two defects into account, with  $i = 1, 2$ . Furthermore, the average emission times of each defect are given by  $\tau_i$ . The p.d.f. of having an emission event from each of these defects is then

$$P_i(t) = p_i f(t; \tau_i) \quad (2)$$

where  $f(t; \tau_i)$  is the exponential distribution with characteristic emission time  $\tau_i$ . Note that  $P_i(t)$  is normalized to  $p_i$  rather than unity. Under the assumption that both defects emit a hole, the p.d.f. for the event  $t_a = \min(t_1, t_2)$  is

$$P_a^0(t) = \int_t^\infty P(t, t_2) dt_2 + \int_t^\infty P(t_1, t) dt_1 = f(t; \tau) \quad (3)$$

using the joint p.d.f. of the independent processes  $P(t_1, t_2) = f(t_1; \tau_1)f(t_2; \tau_2)$  and  $1/\tau = (1/\tau_1 + 1/\tau_2)$ . Then, for the general case of  $p_i \leq 1$ , we obtain

$$P_a(t) = P_1(t) + P_2(t) - P_b(t), \quad (4)$$

$$P_b(t) = p_2 P_1(t) + p_1 P_2(t) - p_1 p_2 P_a^0(t). \quad (5)$$

The distributions  $P_a$  and  $P_b$  are shown in Fig. 4 for varying  $\tau_2$ . As will become clear later, the distribution of the random variable  $\Delta t = t_2 - t_1$  is also of interest.

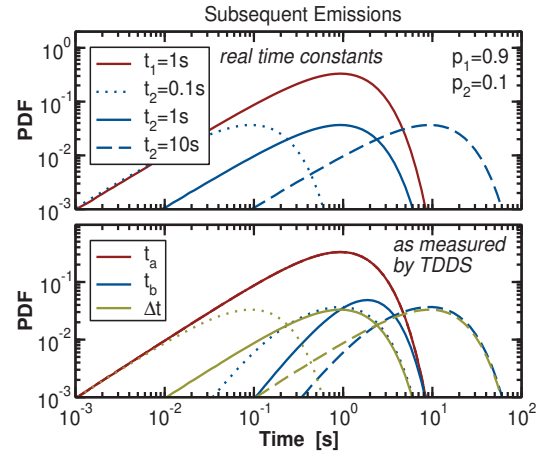


Fig. 5: Scenarios B/C: **Top**: As in Fig. 4, but now for two defects subsequently emitting a hole. **Bottom**: The distribution of the first emission event  $t_a$  recorded by TDDS is of course identical to that of  $t_1$ , while the distribution  $t_b$  is narrower than exponential. Most importantly, however, the distribution of  $\Delta t$  can clearly reveal the case where the second emission event quickly follows the first.

### B. Scenario B: Doubly Charged Defect

In scenario B, we assume that a defect can capture two holes, which are then released subsequently. In this case, we would expect  $t_a = t_1$  and  $\Delta t = t_b - t_a = t_1$  to be independent and exponentially distributed. The resulting distributions are shown in Fig. 5.

### C. Scenario C: Multi-Step Trapping

Finally, in scenario C, we assume that after a certain stress time, the holes hop deeper into the oxide, making space for another hole to be trapped in the original defect. Again, from a statistical perspective, emission would then be like in scenario B. However, we would expect the oxide field to have a strong impact on the probability of onward tunneling, similarly to resonant tunneling structures.

Unfortunately, for scenarios B and C where  $t_1$  and  $\Delta t$  are independent, very similar distributions are obtained, which cannot be distinguished using our small sample size of  $N = 100$  traces. The most marked difference would be the case where the second emission event would quickly follow the first one, which would result in different distributions for  $t_b$  and  $\Delta t$ . So we proceed by extracting  $\tau_1$  and  $\tau_2$  assuming them to be the original emission times of the independent defects using (4) and (5), and check their plausibility later.

## IV. RESULTS AND DISCUSSION

Typical experimental data are shown in Fig. 6, which demonstrates that also  $\tau_2$  can be extracted with satisfactory accuracy. The extracted capture and emission times as a function of bias and temperature are shown in Fig. 7 and Fig. 8. As noted before,  $\tau_1$  and  $\tau_2$  are very similar for all bias conditions and temperatures.

These data can now be compared with the expected predictions of the model scenarios. Before doing so, we briefly summarize general properties of the defects responsible for

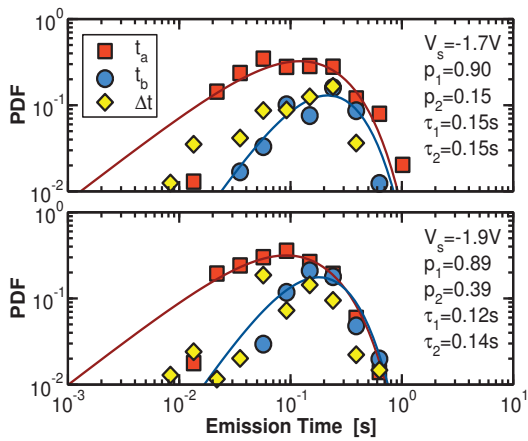


Fig. 6: Typical extraction result for defect A4 obtained after a stress time of 10 s at  $-1.7$  V and  $-1.9$  V at  $125^\circ\text{C}$ . From  $p_i(t_s)$  the capture time constants can be calculated. Even though only 100 repetitions were available, the noise level in the extracted parameters is satisfactory, showing that the distribution of  $\Delta t$  remains close to the distribution of  $t_a$ . While this data do not allow us to distinguish between scenarios A and C, it is inconsistent with scenario B.

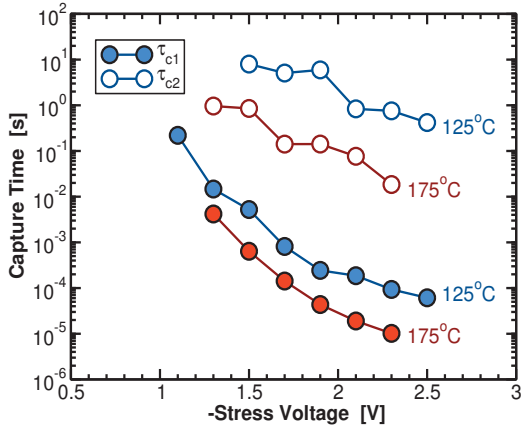


Fig. 7: The extracted capture times  $\tau_{c1}$  and  $\tau_{c2}$  of defect A4 as a function of bias and temperature.  $\tau_{c2}$  is typically 3-4 orders of magnitude larger than  $\tau_{c1}$ .

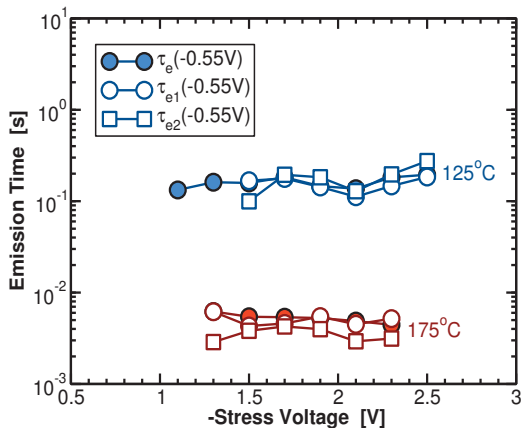


Fig. 8: The extracted emission times  $\tau_1$  and  $\tau_2$  always track each other closely, independently of bias and temperature.

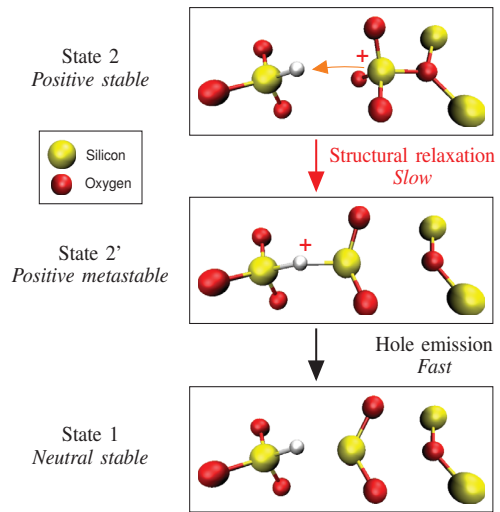


Fig. 9: The emission time constant is dominated by the barrier separating state 2 from state 2', shown above for the hydrogen-bridge in  $\text{SiO}_2$  [14]. Once in state 2', hole emission into state 1 is typically fast for lower biases.

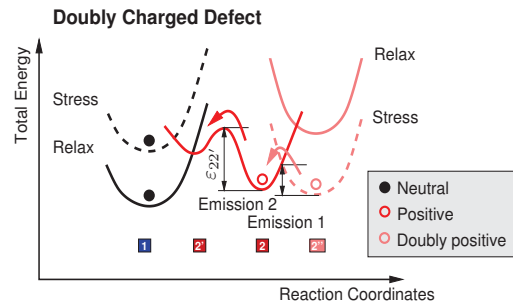


Fig. 10: For a doubly charged defect to produce two emission events with similar emission time constants, the barrier for the non-radiative multiphonon (NMP) [16, 25] transition from the doubly charged state must be similar to the thermal barriers connecting states 2 and 2',  $\epsilon_{22'}$ . As the NMP barrier depends on bias, the occurrence of such a scenario is considered unlikely.

charge trapping in NBTI [15]. Most importantly, it has been observed that hole emission can take much longer than would be expected from an elastic tunneling process due to significant structural relaxation at the defect site [1, 16, 17]. As such, the emission time is often dominated by a relaxation barrier, in our model written as  $\epsilon_{22'}$ , which determines the transition from the stable positive state 2 back to the stable neutral state 1 via a metastable state 2'. While the detailed chemical nature of the defects has not yet been unanimously identified, various forms of the  $E'$  centers have been extensively studied in literature [18–24]. In particular, such large relaxation barriers are often observed for the puckered configuration of  $E'$  centers [14]. While the prototypical  $E'$  center has unfavorable energy levels to be charged during NBTI stress [14], the hydrogen-bridge appears a promising candidate. The three important states for charge emission are shown in Fig. 9, demonstrating the importance of the backward barrier  $\epsilon_{22'}$ .

The main experimental observation is that the two emission times are similar, independently of bias and temperature. This is difficult to reconcile with the doubly charged defect of

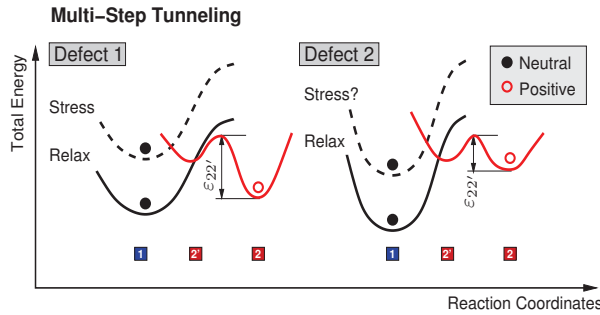


Fig. 11: For a multi-step trapping scenario, the second defect would have to be charged by trapping the hole from the first defect. Assuming a smaller relaxation barrier  $\varepsilon_{22'}$  for defect 2, release would then occur quickly into defect 1 once the hole is emitted from there. Under this assumption, emission would be dominated by the properties of defect 1, possibly explaining the similar emission times. However, as the capture times are dominated by the multiphonon processes and the barriers rather than the tunneling times, it is unclear why such a defect would not directly communicate with the channel.

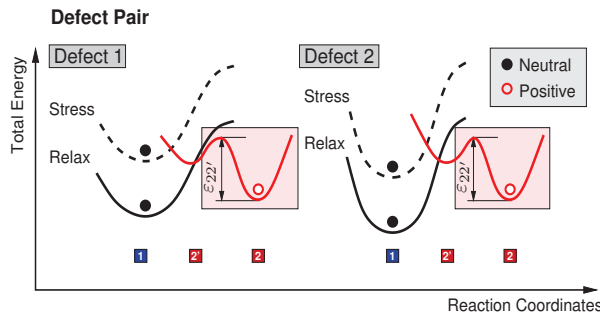


Fig. 12: For two independent defects to incidentally have similar emission time constants, the thermal barriers connecting states 2 and 2',  $\varepsilon_{22'}$ , must be similar. The circumstances for this to happen remain to be clarified.

scenario B, see Fig. 10. Here, we would expect the first hole emission to be strongly bias dependent and fast, while the second would be again dominated by the barrier  $\varepsilon_{22'}$ . This discrepancy could be resolved by a defect which goes through a further structural relaxation with a barrier comparable to  $\varepsilon_{22'}$ . While this is in principle conceivable, no defect with such properties has been reported to the best of our knowledge.

Regarding scenario C, since onward tunneling deeper into the oxide would be expected to depend strongly on the oxide field, we would expect this second trap to be very close to the first trap for this to be consistent with the data. Also, the emission time of defect 2 into defect 1 would have to be much shorter than the emission time of defect 1, for the second emission to come out with the same time constant, see Fig. 11. However, it is unclear how defect 2 would be prevented from directly communicating with the channel.

Finally, in scenario A the barriers  $\varepsilon_{22'}$  would have to be very similar for both defects to explain the observed  $\tau_1(V_G, T) \approx \tau_2(V_G, T)$  behavior, see Fig. 12. As discussed initially, given the wide distribution of defect parameters this is unlikely to happen merely by chance but could be the result of two defects residing in the same defective area sharing some part of their configuration.

## V. CONCLUSIONS

We have observed that in about 10-20% of the defects studied by TDDS two holes can be captured at larger stress times. The two emission events appear independent and exponentially distributed, with similar emission times for all bias conditions and temperatures. We have discussed three possible scenarios including defect pairs, doubly charged defects, as well as multi-step trapping. Given the experimental evidence, we suggest that we are dealing with a spatially and configurationally closely related pair of defects. The possibility of such configurations must be taken into account in the still unresolved identification of the chemical nature of the defects responsible for NBTI [14].

## ACKNOWLEDGMENTS

This work has received funding from the Austrian Science Fund (FWF) project n°23390-N24 and the European Community's FP7 n°261868 (MORDRED).

## REFERENCES

- [1] T. Grasser, H. Reisinger, P.-J. Wagner, W. Goes, F. Schanovsky, and B. Kaczer, "The Time Dependent Defect Spectroscopy (TDDS) for the Characterization of the Bias Temperature Instability," in *Proc. Intl.Rel.Phys.Symp. (IRPS)*, pp. 16–25, May 2010.
- [2] T. Wang, C.-T. Chan, C.-J. Tang, C.-W. Tsai, H. Wang, M.-H. Chi, and D. Tang, "A Novel Transient Characterization Technique to Investigate Trap Properties in HfSiON Gate Dielectric MOSFETs-From Single Electron Emission to PBTI Recovery Transient," *IEEE Trans.Electron Devices*, vol. 53, no. 5, pp. 1073–1079, 2006.
- [3] V. Huard, C. Parthasarathy, and M. Denais, "Single-Hole Detrapping Events in pMOSFETs NBTI Degradation," in *Proc. Intl.Integrated Reliability Workshop*, pp. 5–9, 2005.
- [4] H. Reisinger, T. Grasser, and C. Schlünder, "A Study of NBTI by the Statistical Analysis of the Properties of Individual Defects in pMOSFETs," in *Proc. Intl.Integrated Reliability Workshop*, pp. 30–35, 2009.
- [5] M. Toledano-Luque, B. Kaczer, P. Roussel, T. Grasser, G. Wirth, J. Franco, C. Vrancken, N. Horiguchi, and G. Groeseneken, "Response of a Single Trap to AC Negative Bias Temperature Stress," in *Proc. Intl.Rel.Phys.Symp. (IRPS)*, pp. 364–371, 2011.
- [6] J. Zou, J. Zou, C. Liu, R. Wang, X. Xu, J. Liu, H. Wu, Y. Wang, and R. Huang, "On the Statistical Trap-Response (STR) Method for Characterizing Random Trap Occupancy and NBTI Fluctuation," in *IEEE Silicon Nanoelectronics Workshop (SNW)*, pp. 1–2, June 2012.
- [7] J. Zou, R. Wang, N. Gong, R. Huang, X. Xu, J. Ou, C. Liu, J. Wang, J. Liu, J. Wu, S. Yu, P. Ren, H. Wu, S. Lee, and Y. Wang, "New Insights into AC RTN in Scaled High- $\kappa$ /Metal-gate MOSFETs under Digital Circuit Operations," in *IEEE Symposium on VLSI Technology Digest of Technical Papers*, pp. 139–140, 2012.
- [8] T. Grasser, K. Rott, H. Reisinger, P.-J. Wagner, W. Goes, F. Schanovsky, M. Waltl, M. Toledano-Luque, and B. Kaczer, "Advanced Characterization of Oxide Traps: The Dynamic Time-Dependent Defect Spectroscopy," in *Proc. Intl.Rel.Phys.Symp. (IRPS)*, pp. 2D.2.1–2D.2.7, Apr. 2013.
- [9] T. Grasser, H. Reisinger, K. Rott, M. Toledano-Luque, and B. Kaczer, "On the Microscopic Origin of the Frequency Dependence of Hole Trapping in pMOSFETs," in *Proc. Intl.Electron Devices Meeting (IEDM)*, pp. 19.6.1–19.6.4, Dec. 2012.
- [10] M. Uren, M. Kirton, and S. Collins, "Anomalous Telegraph Noise in Small-Area Silicon Metal-Oxide-Semiconductor Field-Effect Transistors," *Physical Review B*, vol. 37, no. 14, pp. 8346–8350, 1988.
- [11] T. Grasser, K. Rott, H. Reisinger, M. Waltl, P. Wagner, F. Schanovsky, W. Goes, G. Pobegen, and B. Kaczer, "Hydrogen-Related Volatile Defects as the Possible Cause for the Recoverable Component of NBTI," in *Proc. Intl.Electron Devices Meeting (IEDM)*, Dec. 2013.

- [12] H. Reisinger, O. Blank, W. Heinrigs, A. Mühlhoff, W. Gustin, and C. Schlünder, "Analysis of NBTI Degradation- and Recovery-Behavior Based on Ultra Fast  $V_{th}$ -Measurements," in *Proc. Intl.Rel.Phys.Symp. (IRPS)*, pp. 448–453, 2006.
- [13] E. Wu, B. Li, J. Stathis, R. Achanta, R. Filippi, and P. McLaughlin, "A Time-Dependent Clustering Model for Non-Uniform Dielectric Breakdown," in *Proc. Intl.Electron Devices Meeting (IEDM)*, pp. 401–404, Dec. 2013.
- [14] F. Schanovsky, W. Goes, and T. Grasser, "A Detailed Evaluation of Model Defects as Candidates for the Bias Temperature Instability," in *Proc. Simulation of Semiconductor Processes and Devices*, pp. 1–4, 2013.
- [15] T. Grasser, "Stochastic Charge Trapping in Oxides: From Random Telegraph Noise to Bias Temperature Instabilities," *Microelectronics Reliability*, vol. 52, pp. 39–70, 2012.
- [16] C. Henry and D. Lang, "Nonradiative Capture and Recombination by Multiphonon Emission in GaAs and GaP," *Physical Review B*, vol. 15, no. 2, pp. 989–1016, 1977.
- [17] A. Palma, A. Godoy, J. A. Jimenez-Tejada, J. E. Carceller, and J. A. Lopez-Villanueva, "Quantum Two-Dimensional Calculation of Time Constants of Random Telegraph Signals in Metal-Oxide-Semiconductor Structures," *Physical Review B*, vol. 56, no. 15, pp. 9565–9574, 1997.
- [18] A. Lelis and T. Oldham, "Time Dependence of Switching Oxide Traps," *IEEE Trans.Nucl.Sci.*, vol. 41, pp. 1835–1843, Dec 1994.
- [19] E. Poindexter and W. Warren, "Paramagnetic Point Defects in Amorphous Thin Films of  $\text{SiO}_2$  and  $\text{Si}_3\text{N}_4$ : Updates and Additions," *J.Electrochem.Soc.*, vol. 142, no. 7, pp. 2508–2516, 1995.
- [20] J. Conley Jr., P. Lenahan, A. Lelis, and T. Oldham, "Electron Spin Resonance Evidence for the Structure of a Switching Oxide Trap: Long Term Structural Change at Silicon Dangling Bond Sites in  $\text{SiO}_2$ ," *Appl.Phys.Lett.*, vol. 67, no. 15, pp. 2179–2181, 1995.
- [21] P. Blöchl, "First-Principles Calculations of Defects in Oxygen-Deficient Silica Exposed to Hydrogen," *Physical Review B*, vol. 62, no. 10, pp. 6158–6179, 2000.
- [22] D. Fleetwood, H. Xiong, Z.-Y. Lu, C. Nicklaw, J. Felix, R. Schrimpf, and S. Pantelides, "Unified Model of Hole Trapping,  $1/f$  Noise, and Thermally Stimulated Current in MOS Devices," *IEEE Trans.Electron Devices*, vol. 49, no. 6, pp. 2674–2683, 2002.
- [23] P. Lenahan, "Atomic Scale Defects Involved in MOS Reliability Problems," *Microelectronic Engineering*, vol. 69, pp. 173–181, 2003.
- [24] A. Kimmel, P. Sushko, A. Shluger, and G. Bersuker, "Positive and Negative Oxygen Vacancies in Amorphous Silica," in *Silicon Nitride, Silicon Dioxide, and Emerging Dielectrics 10* (R. Sah, J. Zhang, Y. Kamakura, M. Deen, and J. Yota, eds.), vol. 19, pp. 2–17, ECS Transactions, 2009.
- [25] S. Makram-Ebeid and M. Lannoo, "Quantum Model for Phonon-Assisted Tunnel Ionization of Deep Levels in a Semiconductor," *Physical Review B*, vol. 25, no. 10, pp. 6406–6424, 1982.